

UC Irvine

UC Irvine Previously Published Works

Title

Digital holographic microscopy for quantitative cell dynamic evaluation during laser microsurgery

Permalink

<https://escholarship.org/uc/item/8vt2d3hp>

Journal

Optics Express, 17(14)

ISSN

1094-4087

Authors

Yu, Lingfeng
Mohanty, Samarendra
Zhang, Jun
[et al.](#)

Publication Date

2009-07-02

DOI

10.1364/OE.17.012031

Copyright Information

This work is made available under the terms of a Creative Commons Attribution License, available at <https://creativecommons.org/licenses/by/4.0/>

Peer reviewed

Digital holographic microscopy for quantitative cell dynamic evaluation during laser microsurgery

Lingfeng Yu^{1*}, Samarendra Mohanty¹, Jun Zhang¹, Suzanne Genc¹, Myung K. Kim², Michael W. Berns¹ and Zhongping Chen¹

¹Beckman Laser Institute, University of California, Irvine, Irvine, CA 92617

²Dept. of Physics, University of South Florida, Tampa, FL 33620

*yulingfeng@gmail.com

Abstract: Digital holographic microscopy allows determination of dynamic changes in the optical thickness profile of a transparent object with sub-wavelength accuracy. Here, we report a quantitative phase laser microsurgery system for evaluation of cellular/ sub-cellular dynamic changes during laser micro-dissection. The proposed method takes advantage of the precise optical manipulation by the laser microbeam and quantitative phase imaging by digital holographic microscopy with high spatial and temporal resolution. This system will permit quantitative evaluation of the damage and/or the repair of the cell or cell organelles in real time.

©2009 Optical Society of America

OCIS codes: (090.1760) Computer holography; (350.4855) Optical tweezers or optical manipulation; (170.1530) Cell analysis; (090.2880) Holographic interferometry

References and links

1. M. W. Berns, "A history of laser scissors (microbeams)," *Laser Manipulation of Cells and Tissues* **82**, 1–58 (2007).
2. M. W. Berns, R. S. Olson, and D. E. Rounds, "In vitro production of chromosomal lesions with an argon laser microbeam," *Nature* **221**(5175), 74–75 (1969).
3. M. W. Berns, J. Aist, J. Edwards, K. Strahs, J. Girton, P. McNeill, J. B. Rattner, M. Kitzes, M. Hammer-Wilson, L. H. Liaw, A. Siemens, M. Koonce, S. Peterson, S. Brenner, J. Burt, R. Walter, P. J. Bryant, D. van Dyk, J. Coulombe, T. Cahill, and G. S. Berns, "Laser microsurgery in cell and developmental biology," *Science* **213**(4507), 505–513 (1981).
4. S. Monajembashi, C. Cremer, T. Cremer, J. Wolfrum, and K. O. Greulich, "Microdissection of human chromosomes by a laser microbeam," *Exp. Cell Res.* **167**(1), 262–265 (1986).
5. W. Tao, J. Wilkinson, E. J. Stanbridge, and M. W. Berns, "Direct gene transfer into human cultured cells facilitated by laser micropuncture of the cell membrane," *Proc. Natl. Acad. Sci. U.S.A.* **84**(12), 4180–4184 (1987).
6. U. K. Tirlapur, and K. König, "Femtosecond near-infrared laser pulses as a versatile non-invasive tool for intra-tissue nanoprocessing in plants without compromising viability," *Plant J.* **31**(3), 365–374 (2002).
7. G. Palumbo, M. Caruso, E. Crescenzi, M. F. Tecce, G. Roberti, and A. Colasanti, "Targeted gene transfer in eucaryotic cells by dye-assisted laser optoporation," *J. Photochem. Photobiol. B* **36**(1), 41–46 (1996).
8. H. Schneckenburger, A. Hendinger, R. Sailer, W. S. L. Strauss, and M. Schmitt, "Laser-assisted optoporation of single cells," *J. Biomed. Opt.* **7**(3), 410–416 (2002).
9. Y. Shirahata, N. Ohkohchi, H. Itagak, and S. Satomi, "New technique for gene transfection using laser irradiation," *J. Investig. Med.* **49**(2), 184–190 (2001).
10. S. K. Mohanty, M. Sharma, and P. K. Gupta, "Laser-assisted microinjection into targeted animal cells," *Biotechnol. Lett.* **25**(11), 895–899 (2003).
11. R. Wiegand, G. Weber, K. Zimmermann, S. Monajembashi, J. Wolfrum, and K. O. Greulich, "Laser-induced fusion of mammalian cells and plant protoplasts," *J. Cell Sci.* **88**(Pt 2), 145–149 (1987).
12. C. E. Sims, G. D. Meredith, T. B. Krasieva, M. W. Berns, B. J. Tromberg, and N. L. Allbritton, "Laser-micropipet combination for single-cell analysis," *Anal. Chem.* **70**(21), 4570–4577 (1998).
13. Y. Tadir, J. Neev, and M. W. Berns, "Laser in assisted reproduction and genetics," *J. Assist. Reprod. Genet.* **9**(4), 303–305 (1992).
14. M. F. Yanik, H. Cinar, H. N. Cinar, A. D. Chisholm, Y. Jin, and A. Ben-Yakar, "Neurosurgery: functional regeneration after laser axotomy," *Nature* **432**(7019), 822 (2004).

15. J. Colombelli, E. G. Reynaud, J. Rietdorf, R. Pepperkok, and E. H. K. Stelzer, "In vivo selective cytoskeleton dynamics quantification in interphase cells induced by pulsed ultraviolet laser nanosurgery," *Traffic* **6**(12), 1093–1102 (2005).
16. K. F. A. Ross, *Phase Contrast and Interference Microscopy for Cell Biologists* (Edward Arnold Publishers, London, 1967).
17. R. D. Allen, G. B. David, and G. Nomarski, "The Zeiss-Nomarski differential equipment for transmitted light microscopy," *Z. Wiss. Mikrosk.* **69**(4), 193–221 (1969).
18. A. Barty, K. A. Nugent, D. Paganin, and A. Roberts, "Quantitative optical phase microscopy," *Opt. Lett.* **23**(11), 817–819 (1998), <http://www.opticsinfobase.org/ol/abstract.cfm?URI=ol-23-11-817>.
19. E. Cuhe, F. Bevilacqua, and C. Depeursinge, "Digital holography for quantitative phase-contrast imaging," *Opt. Lett.* **24**(5), 291–293 (1999), <http://www.opticsinfobase.org/ol/abstract.cfm?URI=ol-24-5-291>.
20. G. Popescu, L. P. Deflores, J. C. Vaughan, K. Badizadegan, H. Iwai, R. R. Dasari, and M. S. Feld, "Fourier phase microscopy for investigation of biological structures and dynamics," *Opt. Lett.* **29**(21), 2503–2505 (2004), <http://www.opticsinfobase.org/ol/abstract.cfm?URI=ol-29-21-2503>.
21. C. G. Rylander, D. P. Davé, T. Akkin, T. E. Milner, K. R. Diller, and A. J. Welch, "Quantitative phase-contrast imaging of cells with phase-sensitive optical coherence microscopy," *Opt. Lett.* **29**(13), 1509–1511 (2004), <http://www.opticsinfobase.org/ol/abstract.cfm?URI=ol-29-13-1509>.
22. C. J. Mann, L. F. Yu, C. M. Lo, and M. K. Kim, "High-resolution quantitative phase-contrast microscopy by digital holography," *Opt. Express* **13**(22), 8693–8698 (2005), <http://www.opticsinfobase.org/oe/abstract.cfm?URI=oe-13-22-8693>.
23. L. Yu, S. Mohanty, G. Liu, S. Genc, Z. Chen, and M. W. Berns, "Quantitative phase evaluation of dynamic changes on cell membrane during laser microsurgery," *J. Biomed. Opt.* **13**(5), 050508 (2008).
24. A. Khmaladze, M. K. Kim, and C. M. Lo, "Phase imaging of cells by simultaneous dual-wavelength reflection digital holography," *Opt. Express* **16**(15), 10900–10911 (2008), <http://www.opticsinfobase.org/oe/abstract.cfm?URI=oe-16-15-10900>.
25. J. W. Goodman, *Introduction to Fourier Optics* (McGraw-Hill, 1996).
26. R. M. Goldstein, H. A. Zebker, and C. L. Werner, "Satellite radar interferometry: Two-dimensional phase unwrapping," *Radio Sci.* **23**(4), 713–720 (1988).

1. Introduction

Microscope-based laser scissors uses a focused laser beam to alter and/or to ablate cellular and tissue samples, as well as intracellular organelles. It has become an important tool for cell biologists to study the molecular mechanism of complex biological systems [1,2]. For example, cell behavior or embryonic development have been studied by ablation of sub-cellular organelles such as mitotic organelles, nucleoli, mitochondria or other sub-cellular structures [3]. Small sections of chromosomes were segmented to create genetic libraries [4]. Further, cell membranes could be opened by the laser scissors to facilitate drugs or genetic material entering the cell [5–10] and individual cells were fused to obtain specific "hybridoma" clones [11]. The internal constituents of cells were even released for further analysis by laser scissors-induced lysis [12]. Laser scissors are also used in the clinic to improve human in- vitro fertilization [13]. Recently, laser scissors have been utilized to study the process of injury and regeneration in the nervous system [14]. Visualization of transparent microscopic biological specimens such as living cells and their intracellular constituents being manipulated by a laser scissors is difficult using conventional bright-field microscopy. While changes in fluorescently-labeled intracellular structures can be quantitated subsequent to laser microsurgery, the fluorescent labeling methods are known to affect the laser-induced changes, such as the shrinkage rate of microtubules [15].

Although Zernike phase-contrast microscopy [16] and Nomarski differential interference contrast (DIC) microscopy [17] are the most widely used in laser microsurgery systems, quantitative phase imaging is not feasible with these techniques. The ablation of sub-cellular organelles or cells can only be qualitatively evaluated in phase-contrast microscopy since the ablation/alteration due to laser microsurgery normally appears as paling or dark spots since the phase variation is nonlinearly converted into amplitude variation through the use of a phase plate. In DIC microscopy, the changes in the refractive index of the sample are converted into amplitude changes by splitting a polarized beam into two perpendicularly polarized components, which are then recombined to generate a sheared interferogram to give a three-dimensional perception of the object. In both of these techniques, the phase to amplitude conversion is nonlinear and there are significant artifacts in the images, such as the halo in phase contrast microscopy and the disappearance of contrast along the direction

perpendicular to the shear in DIC microscopy. Quantitative phase imaging [18–23] in laser microsurgery is important since it allows the determination of the optical thickness profile change of a transparent organelle or cell with sub-wavelength accuracy. Recently, we reported the use of short-coherence interference microscopy [23] for quantitative cell evaluation during laser microbeam irradiation with an acquisition speed of a few frames per second, which is mainly limited by the requirement of using multiple phase-shifted interferograms to obtain one phase map. This may limit its applications in observing fast cell dynamic changes during laser microsurgery.

Here we report a quantitative phase laser microsurgery (QPLM) system, which takes advantage of the combination of laser scissors and off-axis digital holographic microscopy. Quantitative phase images are recorded during the process of laser microsurgery, and thus, the dynamic change in phase can be continuously evaluated close to the camera speed of 30 frames per second. Digital holographic microscopy also allows numerical reconstruction of dynamic cell movements along the optical axis. The introduction of quantitative phase imaging with laser scissors will make it possible to evaluate quantitatively the damage or the repair of the cell or cell organelle in real time.

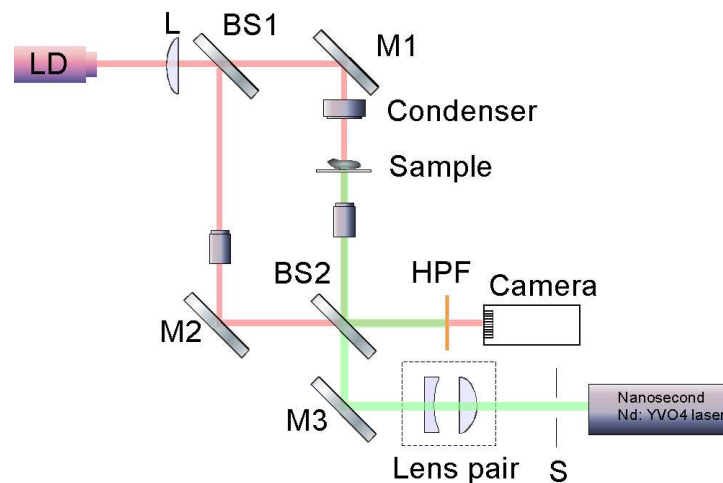


Fig. 1. Schematic of the experimental setup. LD is the 675nm laser diode; BS1 and BS2 are beam splitters; Ms are mirrors; S is a shutter; L is a lens; HPF is a high-pass filter for red light.

2. System setup and results

The design of the quantitative phase laser microsurgery system is described in Fig. 1. After passing through a 5X beam expander, the second harmonic 532 nm green scissor beam from a nanosecond Nd: YVO₄ laser (20KHz, 12 ns, Coherent Inc, USA) is guided through a shutter and a lens pair, deviated by a mirror (M3) and focused onto a small spot in the sample by an objective (40X, 0.65NA). The lens pair, composed of a concave and a convex lens, is introduced to match the focal plane with the imaging plane of the objective. For the purpose of quantitative phase imaging, the red light from a laser diode of 675 nm is focused by a lens, L, and split into a Mach-Zehnder interferometer. The two light beams through the object and the reference arms are directed towards a CCD camera (Sony XCD 710). A 20X objective was placed in the reference arm of the interferometer and the curvature of the interference fringes was digitally compensated and controlled via software [24]. A slight angle is introduced between the object and the reference beams for off-axis holography. The camera has an array of 1024 × 768 pixels with pixel size of 4.65 μm and 8-bit gray scale output with an acquisition speed of 30 frames per second. An IEEE1394 cable connects the camera to the desktop computer, which processes the acquired images and calculates the holographic diffraction using a number of programs based on LabVIEW® in real-time. From Fourier

optics [25], if $E(x, y; 0)$ is the object wave field at plane $z = 0$, the corresponding angular spectrum of the object wave at this plane, $S(k_x, k_y; 0)$, can be obtained by taking the Fourier transform of the hologram and separating it from other spectral components of the hologram with a band-pass filter if the off-axis angle θ of the incident beam is properly adjusted. Here k_x and k_y are corresponding spatial frequencies of x and y . After propagating along the z axis to a new plane, the new angular spectrum, $S(k_x, k_y; z)$, at plane z can be calculated from $S(k_x, k_y; 0)$ as $S(k_x, k_y; 0) \exp[ik_z z]$, where $k_z = [k^2 - k_x^2 - k_y^2]^{1/2}$ and $k = 2\pi/\lambda$. Thus the complex field distribution of any plane z perpendicular to the propagating axis can be calculated by an inverse Fourier transform of $S(k_x, k_y; z)$. The resolution of the reconstructed images from the angular spectrum method is the same as that in the hologram plane. The non-ambiguity phase range calculated from the complex field distribution is only from $-\pi$ to π . Any phase outside this range will cause a wrapping effect of the phase map. The 2π -phase ambiguities can be directly resolved to get an absolute sample phase map by phase unwrapping using Goldstein's algorithm [26].

We present several examples of the quantitative phase laser microsurgery system for evaluation of cellular/ sub-cellular dynamic changes during laser micro-dissection. Figure 2 shows images of rat kangaroo kidney epithelial (PTK2) cells ablated with a laser microbeam. The bright-field image of the cell before the laser microbeam is shown in Fig. 2(a), which shows many chromosomes lying inside the cell. The laser beam was targeted at one spot of the chromosomes as marked with a white arrow in Fig. 2(a). A custom-designed program was used to record holograms in real time and could be triggered to record automatically all of the phase maps of the PTK2 sample before and after laser microsurgery. With a pulse frequency of 20 kHz, the average power of the laser microbeam coming out of the 40X objective was measured to be 8 mW, which corresponds to 0.4 μJ / pulse. With a pulse width of 12 ns, this corresponds to a peak irradiance of $2.67 \times 10^9 \text{ W} / \text{cm}^2$. The bright-field image right after the laser microbeam is shown in Fig. 2(b), from which one can observe the defocusing of the chromosomes which could be because of lifting up of the chromosomes. This defocusing may be associated with swelling of the cell. However, from the bright field images, the swelling cannot be confirmed. After about 5 minutes, the defocusing of the chromosomes vanished as shown in Fig. 2(c). Figure 2(d) shows several time-lapse quantitative phase maps of the PTK2 cell during laser microirradiation, assuming the shutter open time as the zero time point. Figure 2(f) also shows a movie of quantitative holographic phase maps of the cell during and after laser microirradiation. The relative phase changes of the cell compared to its original status before laser microirradiation is also given in Figs. 2(e) and 2(g). From the quantitative phase and phase change information, the change in physical thickness of cells can be estimated using the equation $\Delta d = \lambda(\Delta\phi / 2\pi) / (n - n_0)$, where λ is the wavelength, $\Delta\phi$ is the phase, and $(n - n_0)$ is the index difference between the cells and the buffer (or other media). The phase map in Fig. 2(d) ranges from 0 to 3 radians, as indicated in the color bar, which corresponds to an optical thickness span of 6.4 μm , with the assumption of the average index of the cell to be 1.38 and that of the buffer to be 1.33. Though the mechanism for the swelling (by heating and by expansion of the cytoplasm) is still under investigation, the laser-induced swelling can now be quantitatively evaluated. As shown in Fig. 2(e), the maximum phase change of ~ 1.0 radian corresponds to an optical thickness change of 2.1 μm assuming that the refractive index of the cell near the laser microirradiated region does not change. Figure 3 shows the laser micro-dissection of the nucleolus of a PTK2 cell. The laser microbeam is scanned to cut a portion of the nucleolus by manually scanning the mirror (M3). When the laser microbeam is on, we allowed (through the high pass filter) a small portion of the green microbeam to reach the camera so as to enable visualization of the focused spots (shown as bright spots in Fig. 3(b)). If the green microbeam is bright enough to nearly saturate the focused spots in the interferogram, they appear as "singular" (non-smooth) phase points in the

phase map, clearly indicating the ablation/focused laser position, as shown in Fig. 3(d). Note that the ablated nucleolus in Fig. 3 may have a different refractive index from other parts of the cell. To be more accurate, only the phase scale (in radians) is given in Fig. 3. The actual ablation/profile (in microns) can be estimated similarly using a proper estimation of the refractive indices for the cutting spot based on the obtained phase information.

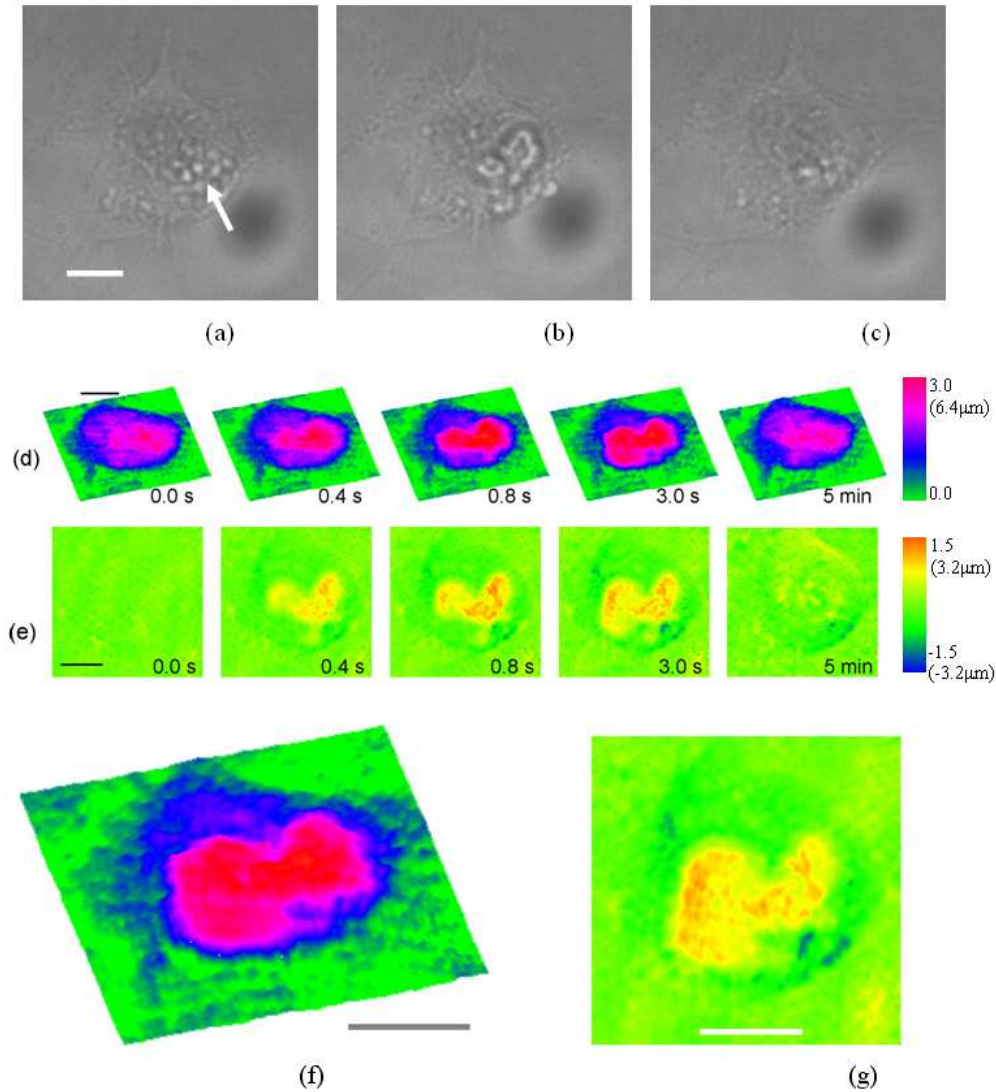


Fig. 2. (Color) Bright-field images of rat kangaroo kidney epithelial (PTK2) cells: (a) Before the laser microbeam; (b) 30 seconds after the laser microbeam; (c) 5 min after the laser microbeam. Figure (d) shows several time-lapse quantitative phase images during the laser microbeam. A time-lapse movie ([Media 1](#)) is shown in (f). Panel (e) shows several time-lapse phase changes of the cell compared to its original status before laser microsurgery and Fig. (g) shows the corresponding movie ([Media 2](#)). Scale bar: 10 μm , $n = 1.38$.

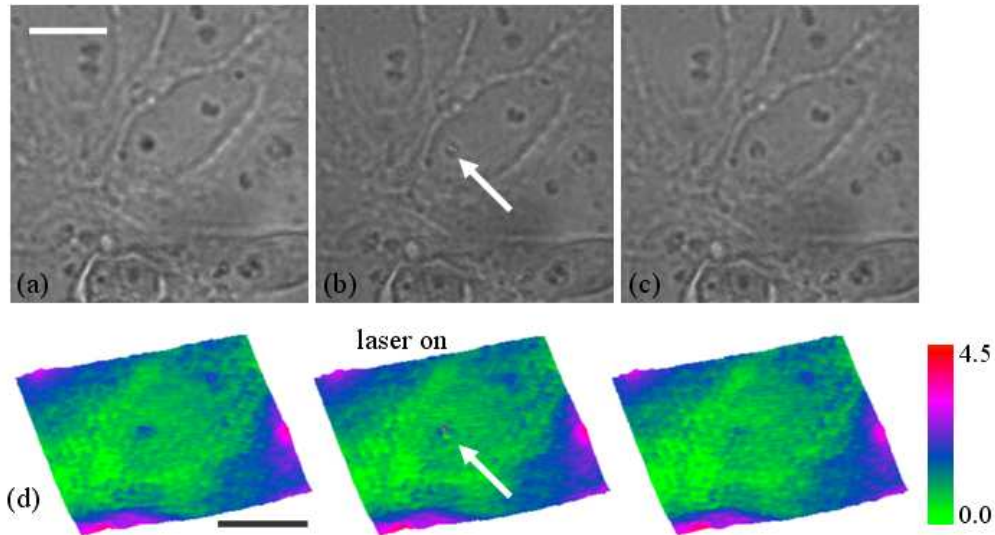


Fig. 3. Bright-field images of PTK2 cell nucleolus: (a) before laser micro-dissection; (b) during laser micro-dissection, with the targeting laser beam on (and passed to the camera) showing the micro-focused spot; (c) after laser micro-irradiation. Figure (d) shows a time-lapse sequence of quantitative phase images (Media 3) during laser microbeam. Scale bar: 10 μm .

Figure 4 shows an example of dynamic microsurgery of red blood cells harvested from a healthy volunteer. The RBCs were separated by centrifugation at 3000 rpm for 10 min and suspended in Phosphate Buffered Saline (pH = 7.4, $n = 1.33$). The RBC suspension was diluted in phosphate buffer (350 mOsm/Kg), spread on a coverslip and observed by the QPLM system. The bright-field image of the crenate RBCs is shown in Fig. 4(a). The position of the laser microbeam in this case is controlled electronically by the mirror (M3) and scanned to cut a straight line across a single RBC. The whole process takes about 4 seconds. Figure 4(b) shows several time-lapse quantitative phase maps of the targeted RBC ablated by the scanning laser microbeam, assuming the ablation starting point as the zero time point. Figure 4(c) shows a movie of quantitative phase changes of the ablated cell.

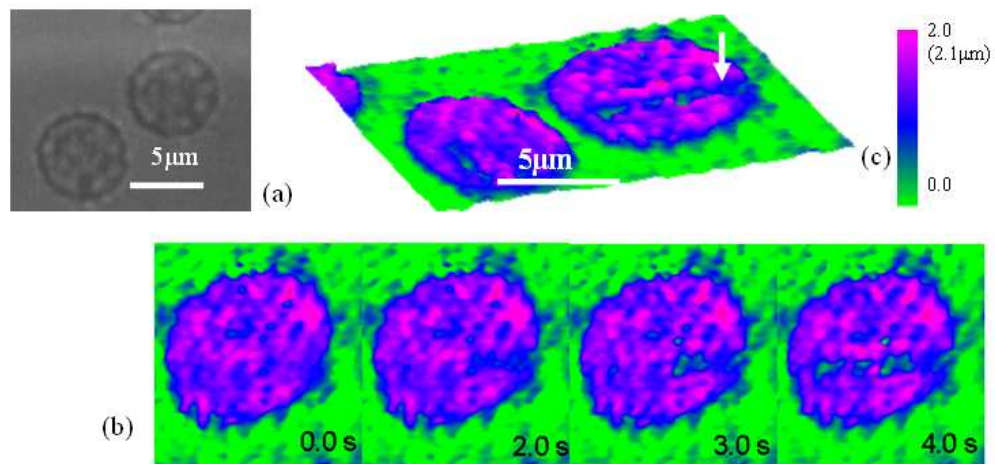


Fig. 4. (Color) (a) Bright-field image of crenate RBC cells; and (b) time-lapse quantitative phase maps of the RBCs during laser microirradiation. Figure (c) shows a movie of quantitative phase images before and during laser microbeam (Media 4). Assuming $n = 1.43$ for crenate RBCs.

Finally in Fig. 5, we show quantitative phase imaging of the response of Goldfish retinal rod cells to green light (laser) exposure. It may be noted that the rod cells in the retina contain photoreceptors that are very sensitive to light, and hence over-exposure of light (as exists in laser microbeams) is expected to cause irreversible damage to the rod cells. Since phase imaging is very sensitive to very subtle changes in the microscopic domain, we should be able to determine the threshold of light required for damaging the rods. For this purpose, we used a low power laser microbeam ($0.1 \mu\text{J}/\text{pulse}$) to hit one end of the rod (as indicated in Fig. 5(a)). The cell membrane of the end was slightly damaged. The rod responded immediately to the irradiation leading to drastic morphological changes. Figures 5(a) and 5(b) show the bright-field images of the rod cell before and after laser irradiation. A time-lapse movie in Fig. 5(c) shows the response of the rod to the laser irradiation and associated morphological changes. Note that our samples are prepared in plastic round chambers with open fluid (buffer). The vibration of the fluid surface will bring some residual phase noise, as is evident in some of the above phase change movies. The system performance could be improved by using closed cell chambers and controlling mechanical vibrations.

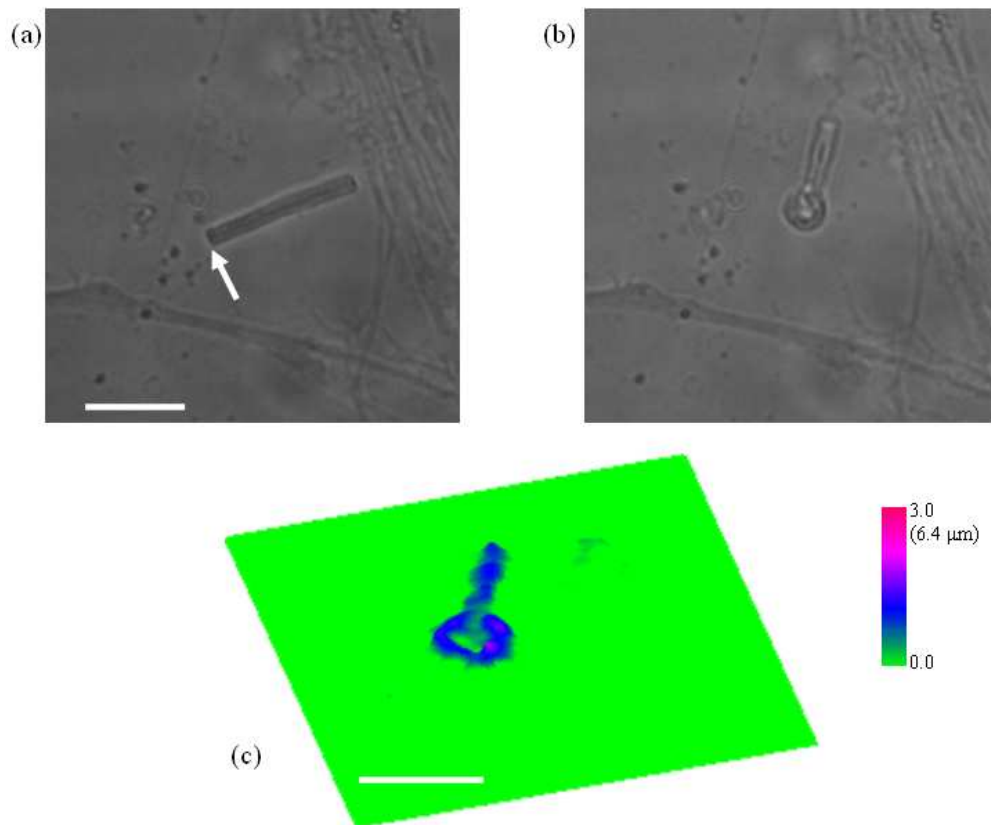


Fig. 5. (Color) Bright-field images of the rod cell from Goldfish retina: (a) Before the laser microbeam; (b) after the laser microbeam; Panel (c) shows quantitative phase change during laser microirradiation (Media 5). Scale bar: $10 \mu\text{m}$, $n = 1.38$.

3. Conclusion

In conclusion, we have demonstrated a quantitative phase laser microsurgery system which takes advantage of the combination of laser scissors and digital holographic microscopy. Quantitative phase images recorded during the process of laser microsurgery of PTK2 cells, goldfish retinal rod cells and human red blood cells allowed evaluation of dynamic changes in

phase in real time. The introduction of quantitative phase imaging in laser microscopy systems would enable quantitative evaluation of the dynamics of damage and/or repair of the cellular structures (such as chromosomes, cell membranes, and neuronal axons) subsequent to laser injury.

Acknowledgments

The Authors would like to thank R. Meyer, J. Miotke and K. Mohanty for providing the Goldfish retinal rods. This work is supported by the National Institutes of Health (EB-00293, CA-91717, RR-01192), and the Air Force Office of Science Research (FA9550-04-1-0101, F9620-00-1-0371). Support from the Beckman Laser Institute Inc. Foundation is also gratefully acknowledged.